An elastoplastic model for structured clays

Bo Chen [*1,2], Qiang Xu [2] and De'an Sun [2,3]

[1] *College of Civil Engineering and Architecture, Quzhou University, Quzhou, 324000, China*
[2] *State Key Laboratory of Geohazard Prevention and Geoenvironmental Protection,*
Chengdu University of Technology, Chengdu, 610059, China
[3] *Department of Civil Engineering, Shanghai University, Shanghai, 200072, China*

Abstract. An elastoplastic model for structured clays, which is formulated based on the fact that the difference in mechanical behavior of structured and reconstituted clays is caused by the change of fabric in the post-yield deformation range, is present in this paper. This model is developed from an elastoplastic model for overconsolidated reconstituted clays, by considering that the variation in the yield surface of structured clays is similar to that of overconsolidated reconstituted clays. However, in order to describe the mechanical behavior of structured clays with precision, the model takes the bonding and parabolic strength envelope into consideration. Compared with the Cam-clay model, only two new parameters are required in the model for structured clays, which can be determined from isotropic compression and triaxial shear tests at different confining pressures. The comparison of model predictions and results of drained and undrained triaxial shear tests on four different marine clays shows that the model can capture reasonable well the strength and deformation characteristics of structured clays, including negative and positive dilatancy, strain-hardening and softening during shearing.

Keywords: structured clay; reconstituted clay; bonding; fabric; elastoplastic model

1. Introduction

The Cam-clay model (Roscoe and Burland 1968, Roscoe *et al.* 1963), which was developed on the mechanical behavior of reconstituted clays, has been widely implemented in finite element programs, on account of its capacity to capture the main mechanical behavior of reconstituted clays. However, it cannot properly predict the strength and deformation characteristics of natural sedimentary clays due to the effect of soil structure, which has important impacts on the mechanical behavior of the clays. Many research results have shown that the mechanical behavior of natural clays is different from that of reconstituted clays (Burland 1990, Leroueil and Vaughan 1990, Nagaraj *et al.* 1990, Cotecchia and Chandler 2000). Therefore, an elastoplastic constitutive model, which can describe reasonably well the strength and deformation characteristics of structured clays, is needed in the engineering application.

With a better understanding of the mechanical behavior of natural clays, much progress has been achieved recently on the constitutive models that can rationally describe the mechanical behavior of structured clays (Asaoka *et al.* 2000, Rouainia and Muir wood 2000, Liu and Carter

---

∗Corresponding author, Lecturer, E-mail: chenbo20020178@163.com

2002, Baudet and Stallebrass 2004). However, most of them are proposed based on the assumption that the mechanical behavior of natural clays can be regarded as a combination of the behavior of the corresponding reconstituted clays and the soil structure effects. With the degradation of soil structure, the mechanical behavior of natural clays will approach that of reconstituted clays, which is termed the intrinsic property of clays by Burland (1990). According to the above considerations, the existing elastoplastic models for structured clays are usually developed as follows: an additional yield surface-named structural yield surface-is introduced outside the yield surface of reconstituted clay, which is also regarded as the reference yield surface, and the relation between structural yield surface and reference yield surface is linked by a structural parameter, which reflects and controls the rate of destructuration of soil structure (Asaoka *et al*. 2000, Rouainia and Muir wood 2000, Baudet and Stallebrass 2004).

The above method to develop elastoplastic constitutive models for structured clays is simple and convenient, but it is assumed that the fabrics of structured and reconstituted clays are almost the same and the difference between them is only caused by the bonding of soil structure. However, our test results obtained from four undisturbed and reconstituted marine clays show that when the consolidation stress is larger than the structural yield stress, most of bonding is broken and the differences in strength and deformation characteristics between undisturbed and reconstituted clays are caused by the difference in the fabric (Chen 2012). The detailed test results will be introduced in the next section. On account of the above observations, the model for structured clays should be developed based on the strength and deformation characteristics of undisturbed clays, and the model parameters should be obtained from the test results of undisturbed clays rather than reconstituted clays.

In this paper, an elastoplastic model for structured clays is presented, which is formulated on the fact that the difference in the mechanical behavior between structured and reconstituted clays is caused by the change of fabric, and the classic critical state theory can also be applicable to structured clays in the post-yield deformation range. This model for structured clays is developed from a model for overconsolidated reconstituted clays (Yao *et al*. 2012) based on the fact that the variation in the yield surface of structured clays is similar to that of reconstituted clays. However, in this new model, the bonding strength present in structured clays is taken into consideration, and the corresponding parabolic strength envelope of overconsolidated reconstituted clays, which was proposed by Yao *et al*. (2012), is further modified to fit the strength envelope of structured clays. The comparison of predicted results by the model and the results of consolidated-drained and undrained triaxial shear tests shows that the model can capture reasonably well the strength and deformation characteristics of structured clays, including negative and positive dilatancy, strain-hardening and softening of structured clays during shearing.

2. Mechanical behavior of structured clays

Many research results have shown that the soil structure has an important effect on the mechanical behavior of clays (Burland 1990, Leroueil and Vaughan 1990, Nagaraj *et al*. 1990, Cotecchia and Chandler 2000, Hong *et al*. 2006), but there are different opinions about the degradation of soil structure. Nagaraj *et al*. (1990) deduced that the soil structure is degraded gradually, based on the fact that the compression curve of undisturbed clay converges slowly to the compression curve of reconstituted clay in the post-yield deformation range; Hong *et al*. (2006) deduced that if the consolidation stress is larger than the structural yield stress, the soil

structure will disappear completely, based on the results of consolidated-undrained triaxial shear tests on reconstituted and undisturbed Ariake clays. Hence, it is necessary to study further the destructuration of structured clays.

With the objective of studying the destructuration of soil structure, a number of isotropic compression and triaxial shear tests on four different marine clays, taken from Hongqiao, Pudong and Pujiang areas in Shanghai, China and Suzhou city, located at 80 km far from Shanghai, have been carried out on undisturbed samples with different sampling methods and corresponding reconstituted samples. The detailed sampling methods are as follows: Pujiang clay was taken by block sampling method, Hongqiao and Suzhou clays were taken by thin wall sampling and Pudong clay was taken by thick wall sampling. Because it is difficult to evaluate quantitatively the soil structure and that all the clays have a soil structure whether they are in intact, destructured or remolded state, the soil structure is simply divided into the fabric and bonding, which can be taken into account respectively (Mitchell 1976). In other words, fabric and bonding are two different elements of the soil structure. The bonding is a meta-stable element while the fabric is a relatively stable element of soil structure (Burland 1990, Baudet and Stallebrass 2004).

The techniques for direct measurement of fabric has not yet been developed, this paper introduces a reference void ratio e_{10}^*, defined by the void ratio at the effective stress of 10 kPa, by extrapolating the virgin compression curve, as shown in Fig. 1. This parameter is used as a soil fabric index to represent the fabric simply. When the results of isotropic compression and triaxial shear tests on four different marine clays are arranged with the reference void ratio e_{10}^*, it is surprising to find that all the post-yield compression and shear test results of undisturbed and corresponding reconstituted clays fall on two unique "master curves", as shown in Figs. 2 and 3, respectively. In these figures, R^2 is the correlation coefficient.

Fig. 2 shows the relationship between compression index C_c from the post-yield compression curve and reference void ratio e_{10}^*. It is found that the undisturbed and reconstituted samples of four different clays have almost the same relation, which could be expressed as the straight line with a high correlation coefficient as Eq. (1).
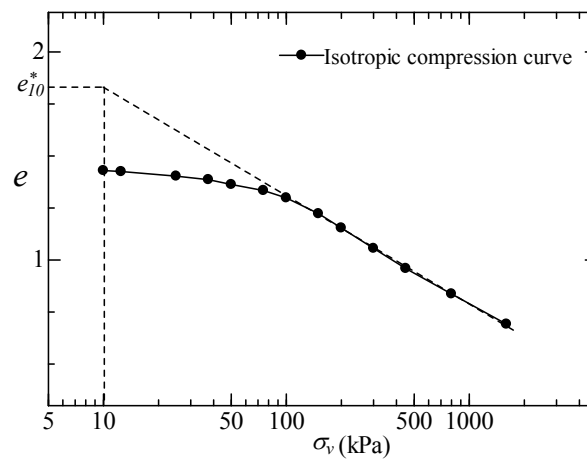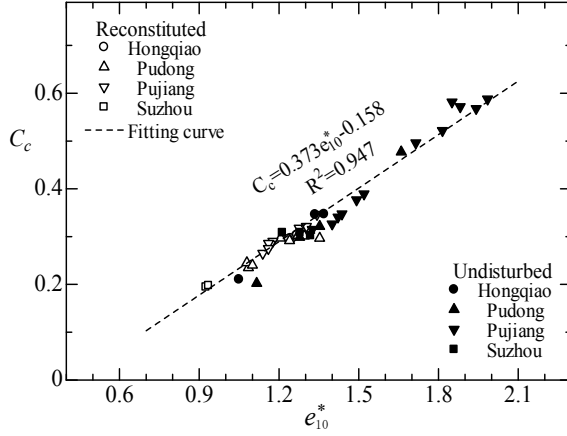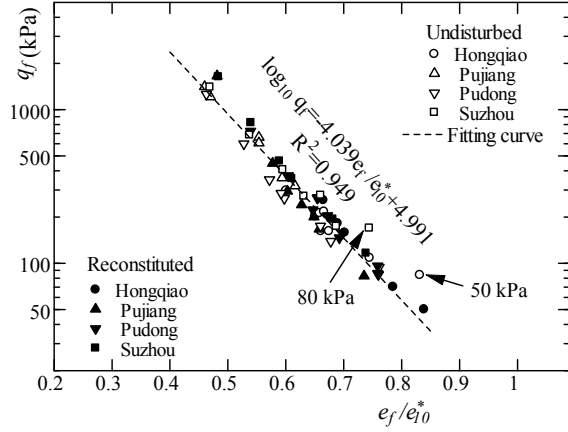
$$C_c = 0.373e_{10}^* - 0.158 \tag{1}$$

Fig. 1 Definitions of reference void ratio e_{10}^*

Fig. 2 C_c-e_{10}^* curves of four different clays   Fig. 3 e_f/e_{10}^*-$\log_{10} q_f$ curves of four different clays

It means that the same relation holds between C_c and e_{10}^* both on undisturbed and reconstituted clays. Hence the fabric of both clays can be indexed by the parameter e_{10}^* about compression behavior.

According to the results of triaxial shear tests on the four undisturbed and reconstituted clays, the shear strength q_f is also plotted against the ratio of void ratio e_f at critical state to the reference void ratio e_{10}^*, as shown in Fig. 3. It is also found that the undisturbed and reconstituted samples of four different clays have the same relation, except for two test data (marks □ and ○). The relation could be expressed by a straight line in the plane (e_f/e_{10}^*, $\log q_f$) with a high correlation coefficient as Eq. (2).

$$\log_{10} q_f = -4.309 e_f / e_{10}^* + 4.991 \tag{2}$$

The two test data (marks □ and ○) in Fig. 3 show a slight deviation from the linear relation, which is caused by the structure bonding. The two test results are from consolidated-undrained triaxial shear tests at the confining pressures of 50 and 80 kPa, respectively, which are lower than the structural yielding stress, and thus the bonding may not be broken down completely at failure.

Based on the test results shown in Figs. 2-3, it can be conjectured that when the confining pressure is larger than the structural yielding stress, most of the bonding is broken and the differences in compression and shear strength characteristics between undisturbed and reconstituted clays are mainly caused by the difference in the fabric. Correspondingly, the framework of constitutive model for structured clays should be similar to that of reconstituted clays during the post-yield loading, the model parameters should be obtained from the test results of undisturbed clays rather than reconstituted clays. During the pre-yield loading, the bonding should be taken into consideration in the model for structured clays.

3. Variation in yield surface of structured clays

The variation in the yield surface of structured clays with the increase of isotropic compression can be illustrated by a schematic diagram, as shown in Fig. 4. It can be seen that undisturbed clay

has an initial structural yield surface whose shape is similar to the yield surface of reconstituted clay, which is termed as intrinsic yield surface (Cotecchia and Chandler 2000), and the shape of structural yield surface will not change during the degradation of structure (Baudet 2001). For simplicity, the shape of structural yield surfaces at different stress states is assumed to be the same as the yield surface of the modified Cam-clay model in the p–q plane (Cotecchia and Chandler 2000, Liu and Carter 2002, Baudet and Stallebrass 2004, Suebsuk *et al.* 2011). Here p and q are mean effective stress and deviator stress, respectively.

In Fig. 4, point 1 represents the initial state in situ for structured clays and the initial structural surface is defined by the structural yield stress p_s and bonding strength p_r, for it doesn't experience any degradation of structure. As loading increases along stress path 1-2-3, where the loading is lower than the structural yield stress p_s, the current loading surface is lying within the initial yield
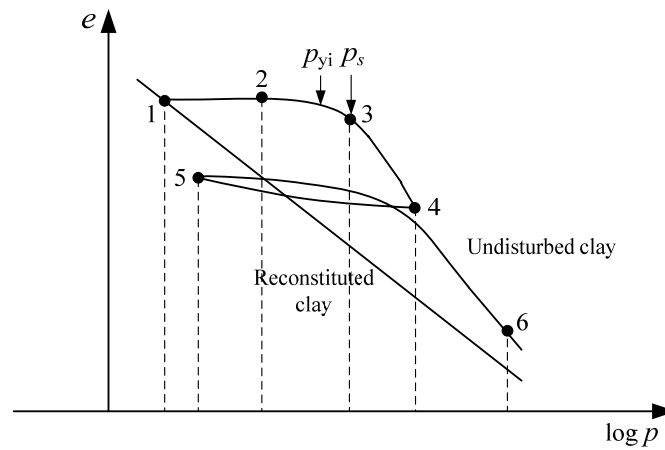
(a) e-log p plane
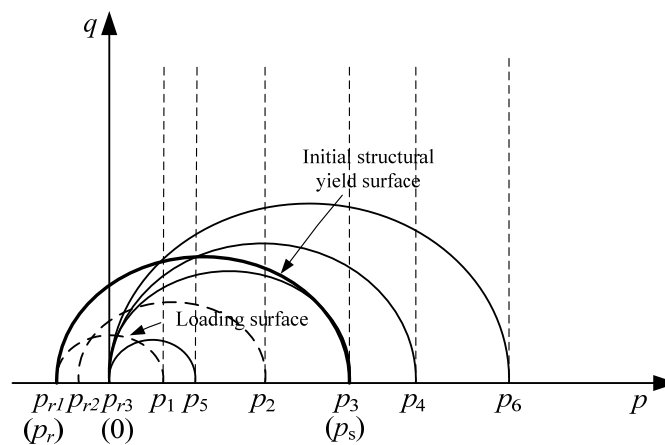
(b) Change in yield surface

Fig. 4 Yield surfaces with change in loading

surface and it is defined by the confining pressures p_2, p_3 and bonding strength p_{r2}, p_{r3} (= 0). The current loading surface will expand with increase of loading and coincides with the initial structural surface at point 3. At the same time, the bonding strength p_r decreases with increase of loading and disappears completely at point 3. As the loading evolves along stress path 3-6, the current loading surface will coincide with the structural yield surface, the latter being defined by a surface passing through the corresponding confining pressures and the origin of the coordinate axes. It should be noted that the bonding strength cannot be recovered with unloading. Therefore, during an isotropic decompression along the path 4-5, the corresponding loading surface goes inside the structural yield surface but passes through the origin of the coordinate axes.

The analysis of the variation in the structural yield surface and current loading surface with the loading of isotropic compression shows that, for structured clays, when the confining pressure is lower than the initial structural yield stress, the change in yield surface is similar to that of overconsolidated reconstituted clays; when the confining pressure is higher than the initial structural yield stress, the change in yield surface is similar to that of normally consolidated clays. Furthermore, the test results of Winnipeg clay, carried out by Graham and Li (1985), show that the features of critical state soil mechanics can be applicable to undisturbed clays, despite some differences in details. Therefore, the elastoplastic model for structured clays could be developed on the basis of the model for overconsolidated reconstituted clays.

On account of the above discussion on the mechanical behavior and the variation in the yield surface of structured clays, it can be concluded that the mechanical behavior of structured clays is similar to that of overconsolidated reconstituted clays at the pre-yield while it is similar to normally consolidated reconstituted clays at the post-yield. Yao *et al*. (2009, 2012) have proposed a unified hardening model that can capture well the mechanical behavior of overconsolidated reconstituted clays and the model is reduced to the Cam-clay model with the complete loss of overconsolidation ratio. Therefore, it is introduced to develop the new model for structured clays. However, in order to model satisfactorily mechanical behavior of structured clays, some improvements on the model for overconsolidated reconstituted clays proposed by Yao *et al*. (2009, 2012) appear necessary. The details are as follows: (1) the bonding strength existing in structured clays is taken into account in the new model; and (2) the parabolic strength envelope is further modified to fit the strength envelope obtained from the test results of structured clays.

4. Constitutive model

4.1 Yield surface and overconsolidated parameter R

When the confining pressure is lower than the initial structural yield stress, there is a current loading surface inside the initial structural yield stress, as shown in Fig. 5. The initial structural yield surface and current loading surface are all similar to the yield surface of the Modified Cam-clay in shape in the *p–q* plane, but they don't pass through the origin of the coordinate axes because the bonding strength exists in the structured clays. There are some differences in the hardening parameter between the initial structural yield surface and current loading surface. For the initial structural yield surface, the hardening parameter is the same as that of the Modified Cam-clay model, i.e., the plastic volumetric strain ε_v^p. For the current loading surface, the hardening parameter is a unified hardening parameter denoted by *H*, which was proposed by Yao *et al*. (2009). Details of the unified hardening parameter *H* will be given later. The initial structural
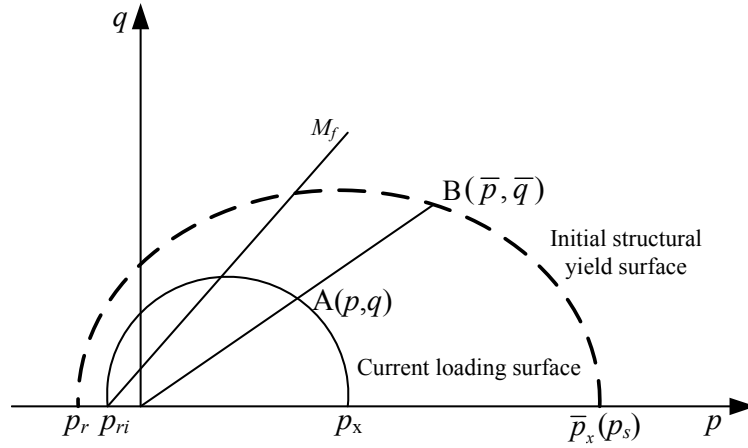
Fig. 5 Current Loading surface and initial structural yield surface

yield surface $\bar{f}$ and current loading surface f can be expressed by Eqs. (3)-(4), respectively.

$$\bar{f} = \ln\frac{\bar{p} + p_r}{\bar{p}_x + p_r} + \ln\left(1 + \frac{\bar{q}^2}{M^2(\bar{p} + p_r)^2}\right) - \frac{1}{c_p}\varepsilon_v^p = 0 \qquad (3)$$

$$f = \ln\frac{p + p_{ri}}{p_x + p_{ri}} + \ln\left(1 + \frac{q^2}{M^2(p + p_{ri})^2}\right) - \frac{1}{c_p}H = 0 \qquad (4)$$

Where $\bar{p}_x$, p_x are respectively the intersections of the initial structural yield surface and current loading surface with the p-axis. p_x is equal to the confining pressure under isotropic compression stress condition at initial stage; $\bar{p}_x$ is equal to the initial structural yield stress p_s when the confining pressure is lower than the initial structural yield stress, while it is equal to the stress p_x, i.e., the confining pressure under isotropic compression stress condition, when the confining pressure is larger than the initial structural yield stress; p_r and p_{ri} are the intersections of the initial yield surface and current loading surface with the p-axis in the rang of $p < 0$; $\bar{p}, \bar{q}$ are the mean stress and deviatoric stress on the initial structural yield surface, respectively; p, q are the mean stress and deviator stress on the current loading surface, respectively; $c_p = (\lambda - \kappa)/(1 + e_0)$; λ, κ are the compression and swelling slopes of e-ln p curve obtained from isotropic compression and unloading tests on undisturbed clays, respectively. e_0 is the initial void ratio, and M is the critical state stress ratio of undisturbed clays.

As suggested by Baudet and Stallebrass (2004), both plastic volumetric and shear strains influence the degradation of structure. By considering the following two reasons, the bonding strength p_r can be evaluated by Eq. (5).

When the confining stress is equal to the structural yield stress p_s, the bonding strength existing in undisturbed clays is almost destructured completely. For simplify, the bonding is assumed to be destructured completely when the stress is equal to or larger than the structural yield stress p_s.

When the confining stress is lower than the structural yield stress, the degradation of bonding

strength can be expressed by the plastic deviator strain ε_s^p, as suggested by Suebsuk *et al.* (2011).

$$p_{ri} = p_r \langle \log(p_s / p) \rangle \exp(-\varepsilon_s^p) \tag{5}$$

Where, $\langle \ \rangle$ is the Macauley bracket, and it means

$$\langle x \rangle = \begin{cases} x & if \ x \geq 0 \\ 0 & if \ x < 0 \end{cases} \tag{6}$$

The relationship between the initial structural yield stress and current loading surface can be linked by an overconsolidation parameter R, which is defined as the ratio of the stress on the current loading surface to the corresponding stress on the initial structural yield stress, as shown in Fig. 5, the equation can be expressed as follows

$$R = p / \overline{p} = q / \overline{q} \tag{7}$$

From Eq. (3), $\overline{p}$ can be written as

$$\overline{p} = (\overline{p}_x + p_r)\left(\frac{M^2}{M^2 + \eta^2}\right)\exp\left(\frac{\varepsilon_v^p}{c_p}\right) - p_r \tag{8}$$

Substituting Eq. (8) into Eq. (7), R can be written as

$$R = p / \overline{p} = p / \left((\overline{p}_x + p_r)\left(\frac{M^2}{M^2 + \eta^2}\right)\exp\left(\frac{\varepsilon_v^p}{c_p}\right) - p_r\right) \tag{9}$$

It can be seen from Eq. (9) that the overconsolidation parameter R is related to the current stress, structural yield stress, bonding strength, etc., and with the increase of compression and shear, R will increase up to the critical state ($R = 1$).

4.2 Potential failure stress ratio M_f

In order to represent the potential capacity in resisting shear failure of overconsolidated reconstituted clays, Yao *et al.* (2009) introduced a potential failure stress ratio M_f, which is related to the overconsolidation parameter R and the slope of the Hvorslev envelope M_h, as shown in Fig. 6, into the model for overconsolidated reconstituted clays. Yao *et al.* (2012) modified the straight Hvorslev envelope by a parabolic Hvorslev envelope passing through the origin of *p-q* plane subsequently, for the purpose to make the model describe the strength characteristics of highly overconsolidated reconstituted clays better, as shown in Fig. 6.

The parabolic Hvorslev envelope is deduced on the fact that overconsolidated reconstituted clay has no cohesion to sustain the tensile stress. However, the cohesion actually exists in structured clays due to soil structure, which was formed during the very slow deposition process. Therefore, the parabolic Hvorslev envelope for overconsolidated reconstituted clays needs to be further modified to fit the mechanical behavior of structured clays. Many test results of structured

Fig. 6 Hvorslev and modified Hvorslev envelopes for reconstituted and structured clays

clays have shown that the strength envelope of structured clays is similar but above the Hvorslev envelope, which describes the strength characteristics of overconsolidated reconstituted clays well (Burland 1990, Callisto and Rampello 2004), as shown in Fig. 6. Consequently, the parabolic strength envelope of structured clays can be modified as follows.

The equation of the modified parabolic strength envelope curve of structured clays is the same as that suggested by Yao *et al.* (2012), as expressed by

$$(q_f - q_a)^2 = 2\beta(p - p_a) \tag{10}$$

Where the point (p_a, q_a) is the vertex of the parabola, while β is a parameter controlling the curvature.

The conditions to determine the parabolic strength envelope of structured clays are different from that of overconsolidated reconstituted clays. As for structured clays, the parabolic curve goes through the point $(-p_r, 0)$ but not the origin of the p–q plane. Also, the tangent slope of the parabola should be equal to 3 at the point $(-p_r, 0)$ but not at the origin of the p–q plane, as shown in Fig. 6. Finally, considering that the confining pressure being equal to or larger than the initial structural yield stress p_s, the mechanical behavior of undisturbed clays can be described by the Cam-clay model. It means that when the stress is equal to the structural yield stress, the critical state stress ratio of structured clays is equal to M. Therefore, the parabola should pass through the point A (p_s, Mp_s), as shown in Fig. 6.

Based on the above three conditions, the following equations can be obtained.

$$\begin{cases} q_a^2 = -2\beta(p_r + p_a) \\ (\partial q_f / \partial p)\big|_{(-p_r, 0)} = \beta(q_f - q_a) = 3 \\ (Mp_s - q_a)^2 = 2\beta(p_s - p_a) \end{cases} \tag{11}$$

The value of q_f can be solved from Eq. (11) and is expressed as follows

$$q_f = \frac{-M^2 p_s^2}{2(3p_r + 3p_s - Mp_s)} + \sqrt{\frac{3M^2 p_s^2}{(3p_r + 3p_s - Mp_s)}\left(p + p_r + \frac{M^2 p_s^2}{12(3p_r + 3p_s - Mp_s)}\right)} \quad (12)$$

Substituting $p_s = p/R$ into Eq. (12) gives

$$q_f = \frac{-M^2 p^2}{2(3p_r R + 3p - Mp)R} + \sqrt{\frac{3M^2 p^2}{(3p_r R + 3p - Mp)R}\left(p + p_r + \frac{M^2 p^2}{12(3p_r R + 3p - Mp)R}\right)} \quad (13)$$

According to the definition of M_f

$$M_f = \frac{q_f}{p} = \frac{-M^2 p}{2(3p_r R + 3p - Mp)R} + \sqrt{\frac{3M^2}{(3p_r R + 3p - Mp)R}\left(p + p_r + \frac{M^2 p^2}{12(3p_r R + 3p - Mp)R}\right)} \quad (14)$$

4.3 Unified hardening/softening parameter H

In order to describe the positive and negative dilatancy, hardening and softening properties of structured clays when the stress is lower than the structural yield stress, a unified hardening/ softening parameter, which was used for overconsolidated reconstituted clays by Yao *et al.* (2009, 2012), is introduced to the model for structured clays. It contains the potential failure stress ratio M_f, the critical state stress ratio M and the current stress ratio $\eta (= q/(p+p_{ri}))$. The unified hardening parameter is written by

$$H = \int dH = \int \frac{1}{R} \frac{M_f^4 - \eta^4}{M^4 - \eta^4} d\varepsilon_v^p \quad (15)$$

Since dH is always non-negative in the hardening stage, it can be seen from the Eq. (15) that when $0 \leq \eta < M$, $d\varepsilon_v^p > 0$, i.e., negative dilatancy; when $M < \eta < M_f$, $d\varepsilon_v^p < 0$, i.e., positive dilatancy. Since dH is non-positive in the softening stage, $d\varepsilon_v^p < 0$ when $0 \leq \eta < M_f$ and η is slightly higher than M_f, which means the positive dilatancy can be described. Hence, the unified hardening/ softening parameter H can control the negative and positive dilatancy in the hardening stage and the positive dilatancy in the softening stage of structured clays.

In order to apply the model to practical engineering by the finite element method, details of the elastoplastic constitutive tensor D_{ijkl} are needed. The derivation of this tensor is given in Appendix.

5. Comparisons of model prediction with experimental results

5.1 Model parameters and their determination

The model contains six model parameters, i.e., λ, κ, M, v, p_s and p_r. Compared with the Cam-clay model, the parameters p_s and p_r are newly introduced in the proposed model, while the other parameters are the same as those in the Cam-clay model. The model parameters can be determined from isotropic compression tests with loading-unloading process, together with drained and undrained triaxial shear tests on undisturbed samples.
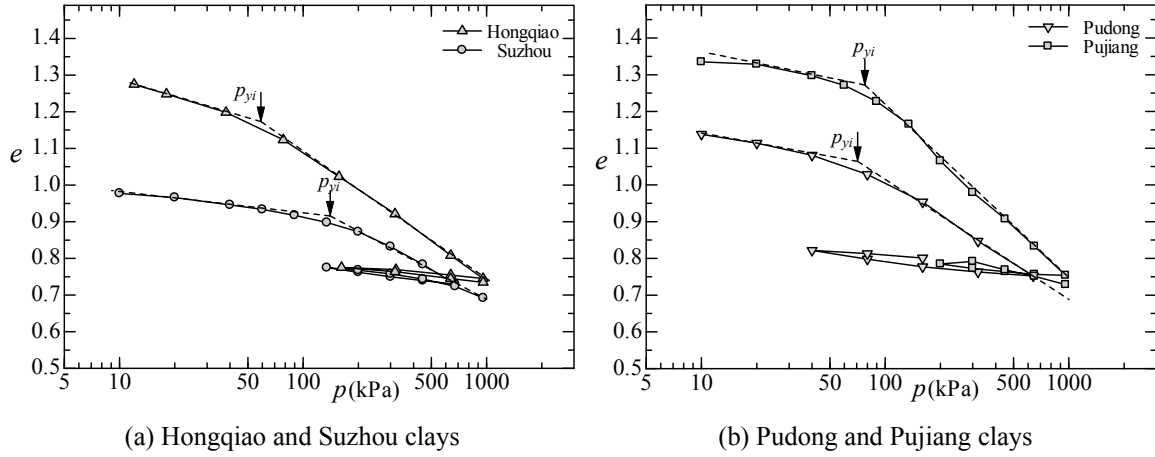
(a) Hongqiao and Suzhou clays

(b) Pudong and Pujiang clays

Fig. 7 Isotropic compression curves of four different undisturbed marine clays

(a) Hongqiao

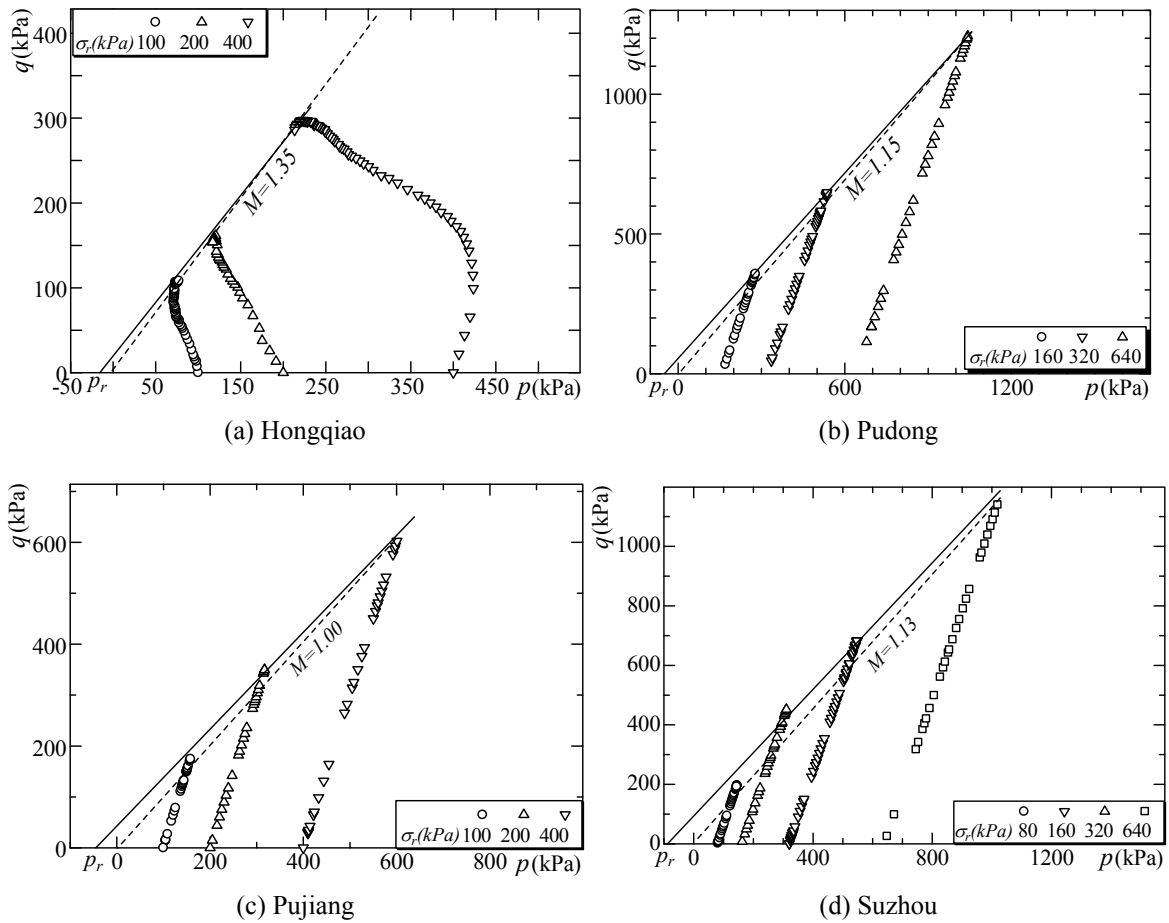(b) Pudong

(c) Pujiang

(d) Suzhou

Fig. 8 Measured stress paths in consolidated-drained triaxial shear tests on four different undisturbed marine clays

Table 1 Model parameters determined from test results of four different clays

Sample name	$\lambda / (1 + e_0)$	$\kappa / (1 + e_0)$	v	p_{yi} (kPa)	M	p_r (kPa)
Hongqiao	0.067	0.009	0.3	59	1.35	16
Pudong	0.062	0.011	0.3	70	1.00	49
Pujiang	0.104	0.017	0.3	77	1.15	44
Suzhou	0.054	0.012	0.3	140	1.13	87

(a) Pudong

(b) Pujiang

(c) Suzhou
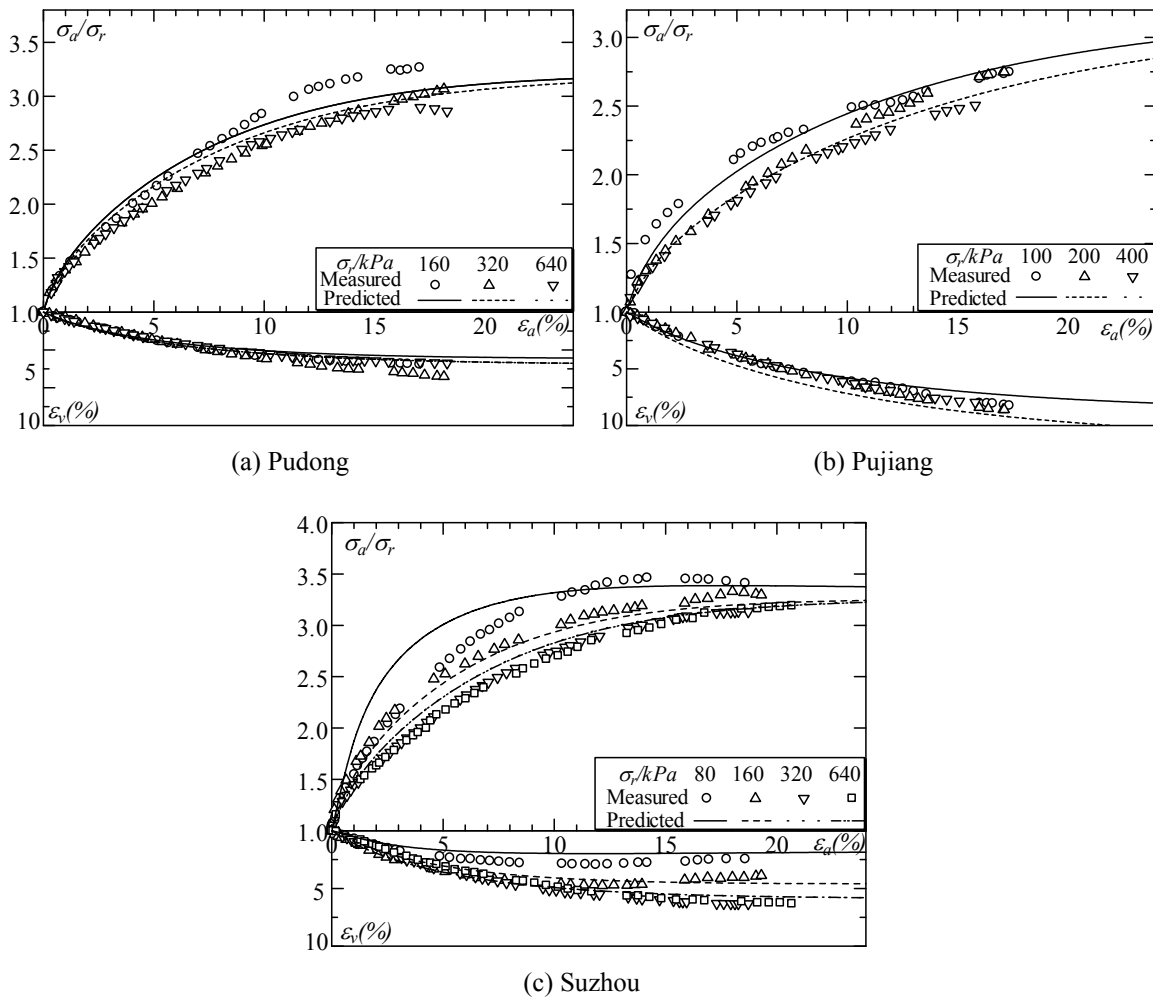
Fig. 9 Comparison between measured and predicted stress-strain curves in consolidated-drained triaxial shear tests

A series of isotropic compression tests, consolidated-undrained and drained triaxial shear tests at different confining pressures were conducted on undisturbed samples of four different clays, i.e., Hongqiao, Pudong, Pujiang and Suzhou clays, which are retrieved by using the thin wall sampling, thick wall sampling, block sampling and thin wall sampling methods, respectively. Hence, the four
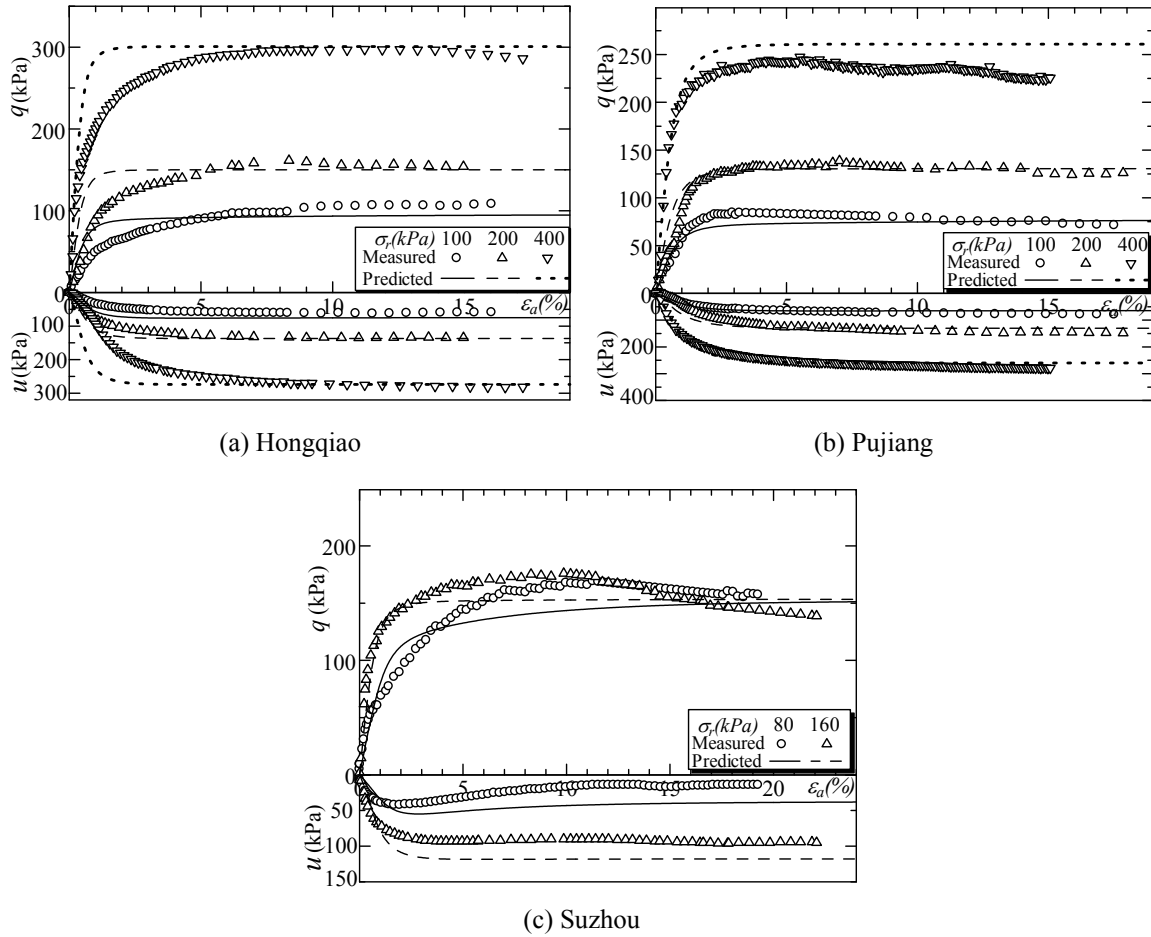
(a) Hongqiao

(b) Pujiang

(c) Suzhou

Fig. 10 Comparison between measured and predicted stress-strain curves in consolidated-undrained triaxial shear tests

samples are subjected to different degrees of disturbance. The plots in Figs. 7-11 show the results of isotropic compression tests and triaxial shear tests on the four samples, respectively.

In details, the model parameters λ, κ and p_s can be determined from the results of isotropic compression tests with unloading stress path, as shown in Fig. 7(a)-(b). The values of parameters λ, κ are 0.434 times the compression indices (c_c) and swell indices (c_s), which are the slopes of compression curves and swell curves, respectively. The value of p_s is 2-3 times the yield stress p_{yi}, which can be obtained by the method suggested by Casagrande (1936), and the detailed relation between p_s and p_{yi} is explained in next paragraph; M and p_r are determined form the results of triaxial shear tests at different confining pressures. The value of M is the critical state stress ratio of undisturbed clay sheared at confining pressures larger than the structural yield stress, p_r is the intersection point of strength envelop with the axial of average principal stress, as shown in Fig. 8; Poisson's ratio v is assumed to be 0.3 in this paper. The detailed values of the relevant model parameters used in predicting the mechanical behavior of four different marine clays are summarized in Table 1.

It should be emphasized that the yield stress determined by the method suggested by Casagrande (1936), denoted by p_{yi}, is lower than the real initial structural yield stress p_s in general, because the undisturbed samples tested have experienced more or less disturbance during the course of sampling, transporting and testing. Hong *et al.* (2012) show that natural clays exhibit the same change in compression behavior compared to reconstituted clays, when the effective stress is 1.0-3.5 times the consolidation yield stress for different undisturbed clays. This means that when the maximum stress experienced 1.0-3.5 times the consolidation yield stress, the soil structure is destructured completely. Some research results (Mesri and Godlewski 1977, Anagnostopoulos and Grammatikopoulos 2011) also show that the secondary consolidation coefficient C_a reaches a maximum value at a stress level about 2-3 times the preconsolidation pressure. Therefore, the value of structural yield stress p_s used in this paper is 2.0, 2.5 and 3.0 times the yield stress determined by the method suggested by Casagrande (1936), denoted as p_{yi}, for undisturbed samples obtained by the block sampling, thin wall sampling and thick wall sampling, respectively. The material parameters used in the model prediction are shown in Table 1.

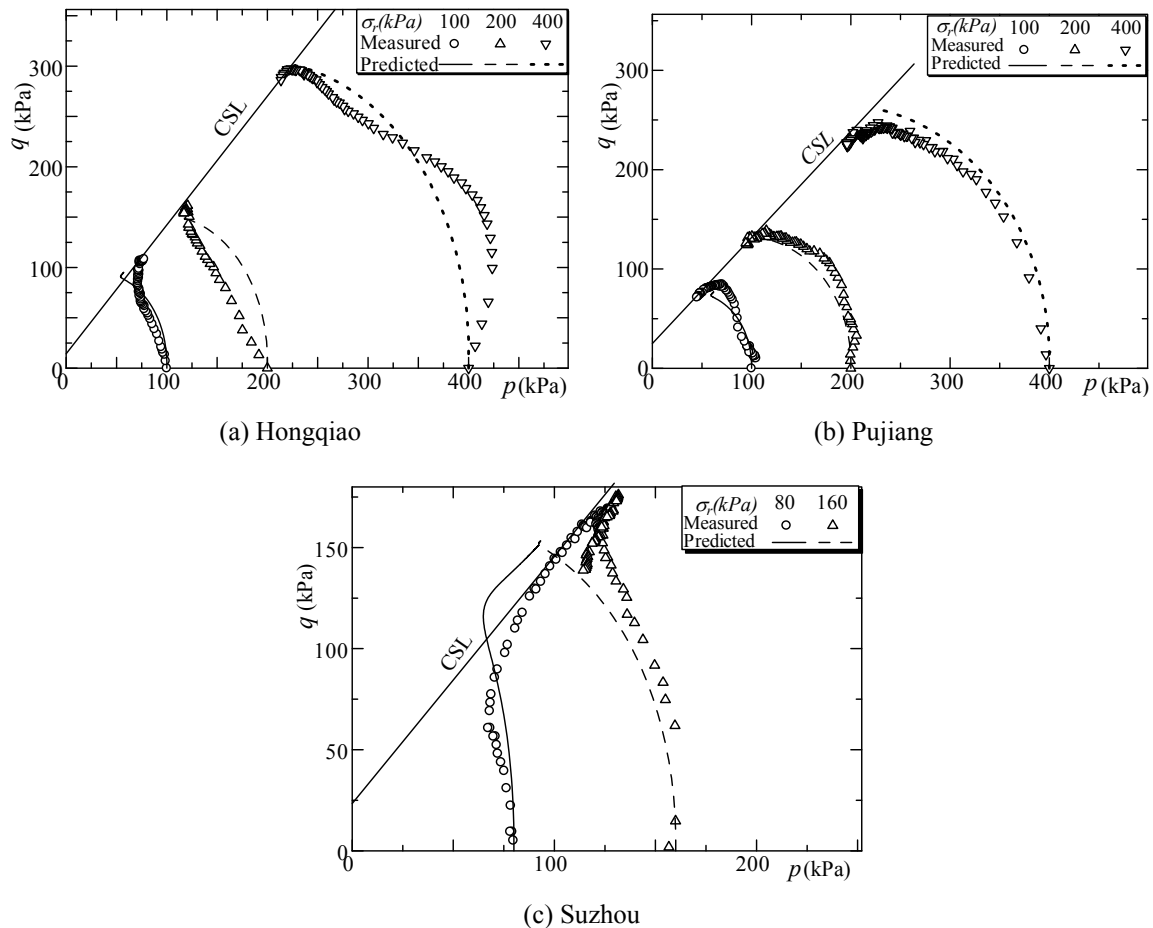(a) Hongqiao

(b) Pujiang

(c) Suzhou

Fig. 11 Comparison between measured and predicted stress paths in consolidated-undrained triaxial shear tests

5.2 Drained triaxial shear test

Fig. 9 shows the measured and predicted stress-strain curves of consolidated- drained triaxial shear tests on Pudong, Pujiang and Suzhou Marine soft clays under different confining pressures. It can be seen that the proposed model can describe well the strength and deformation characteristics of structured clays at different confining pressures. The model prediction shows the negative-dilatancy and strain-hardening characteristics of structured clays when the confining pressure is larger than the initial structural yield stress, as shown in Fig. 9(a), while it shows the positive-dilatancy and strain-softening features of structured clays when the confining pressure is lower than the initial structural yield stress, e.g., the Suzhou marine clay sheared at confining pressure of 80 kPa, as shown in Fig. 9(c).

It should be noted that the two predicted stress-strain curves are converge to one when the confining pressure is larger than the yield structure stress, such as 320 and 640 kPa in Fig. 9(a) and (c), it is because that when the clays are sheared at those confining pressures, they are at normally consolidated state and bonding were broken down completely. Correspondingly, the proposed model for structural clays is degraded to the Cam-clay model and the confining pressure has no effect on the stress ratio-strain curves, as predicted by the Cam-clay model.

5.3 Undrained triaxial shear test

Figs. 10-11 show the measured and predicted stress-strain curves and effective stress paths of consolidated-undrained triaxial shear tests on Hongqiao, Pujiang and Suzhou Marine soft clays under different confining pressures. It can be seen from Figs. 10-11 that the proposed model can predict the excess pore water pressure, stress-path and stress-strain relation of structured clays well under undrained shear condition.

Comparisons between experimental and predicted results shown in Figs. 9-11 demonstrate that the proposed model can predict well the stress-strain curves of natural clays along different stress paths.

6. Conclusions

Based on the analysis of the differences in the mechanical behavior between undisturbed and reconstituted clays and on the variations in the current loading surface and the structural yield surface, an elastoplastic constitutive model for structured clays is presented in this paper. The comparisons of measured and predicted results show that the proposed model gives satisfactory descriptions of the strength and deformation characteristics of four marine structured clays. The main features of this model are:

The bonding strength, which degrades with the plastic volumetric and shear strains, is taken into account in the model. The bonding strength disappears completely when the applied stress reaches several times the consolidation yield stress, based on the test results of four different marine clays.

The parabolic Hvorslev envelope, which was proposed to describe the strength characteristics of overconsolidated reconstituted clays, is further modified to better fit the strength envelope of structured clays.

Compared with the classic Cam-clay model, only two new parameters are required, and they can be derived from isotropic compression test and triaxial drained or undrained shear tests with

different confining pressures.

References

Anagnostopoulos, C.A. and Grammatikopoulos, I.N. (2011), "A new model for the prediction of secondary compression index of soft compressible soils", *Bull. Eng. Geol. Environ.*, **70**(3), 423-427.

Asaoka, A., Nakano, M. and Noda, T. (2000), "Superloading yield surface concept for highly structured soil behavior", *Soil. Found.*, **40**(2), 99-110.

Baudet, B. (2001), "Modelling effects of structure in soft natural clays", Ph.D. Dissertation, City University, London, UK.

Baudet, B. and Stallebrass. S. (2004), "A constitutive model for structured clays", *Géotechnique*, **54**(4), 269-278.

Burland, J.B. (1990), "On the compressibility and shear strength of natural clay", *Géotechnique*, **40**(3), 329-378.

Burland, J.B., Rampello, S., Georgiannou, V.N. and Calabresi, G. (1996), "A laboratory study of the strength of four stiff clays", *Géotechnique*, **46**(3), 491-514.

Callisto, L. and Rampello, S. (2004), "An interpretation of structural degradation for three natural clays", *Can. Geotech. J.*, **41**(3), 392-407.

Casagrande, A. (1936), "The determination of the preconsolidation load and its practical significance", *Proceedings of 1st International Conference on Soil Mechanics and Foundation Engineering*, Boston, MA, USA.

Chen, B. (2012), "Mechanical behavior of soft clay and its elastoplastic modeling", Ph.D. Dissertation, Shanghai University, Shanghai, China.

Cotecchia, F. and Chandler, R.J. (2000), "A general framework for the mechanical behaviour of clays", *Géotechnique*, **50**(4), 431-447

Graham, J. and Li, E.C.C. (1985), "Comparison of natural and remolded plastic clay", *J. Geotech. Eng. Div.*, *ASCE*, **111**(7), 865-881.

Hong, Z.S., Liu, S.Y., Shen, S.L. and Negami, T. (2006), "Comparison in undrained shear strength between undisturbed and remolded Ariake clays", *J. Geotech. Geoenviron. Eng.*, *ASCE*, **132**(2), 272-275.

Hong, Z.S., Zeng, L.L., Cui, Y.J., Cai, Y.Q. and Lin, C. (2012), "Compression behaviour of natural and reconstituted clays", *Géotechnique*, **62**(4), 291-301.

Leroueil, S. and Vaughan, P.R. (1990), "The general and congruent effects of structure in natural soils and weak rocks", *Géotechnique*, **40**(3), 467-488.

Liu, M.D. and Carter, J.P. (2002), "A structured cam clay model", *Can. Geotech. J.*, **39**(6), 1313-1332.

Mesri, G. and Godlewski, P.M. (1977), "Time and stress-compressibility interrelationship", *J. Geotech. Eng.*, *ASCE*, **103**(5), 417-430.

Mitchell, J.K. (1976), *Fundamentals of Soil Behavior*, Wiley, New York, NY, USA.

Nagaraj, T.S., Murthy, B.R.S., Vatsala, A. and Joshi, R.C. (1990), "Analysis of compressibility of sensi- tive soils", *J. Geotech. Eng.*, *ASCE*, **116**(1), 105-118.

Roscoe, K.H. and Burland, J.B. (1968), "On the generalised Stress-strain Behavior of "Wet" Clay", Engineering Plasticity, Cambridge University Press, Cambridge, UK.

Roscoe, K.H., Schofield, A.N. and Thurairajah, A. (1963), "Yielding of clay in states wetter than critical", *Géotechnique*, **13**(3), 211-240.

Rouainia, M., Muir wood, D. (2000), "A kinematic hardening constitutive model for natural clays with loss of structure", *Géotechnique*, **50**(2), 153-164.

Suebsuk, J., Horpibulsuk, S. and Liu, M.D. (2011), "A critical state model for overconsolidated structured clays", *Comput. Geotech*., **38**(5), 648-658.

Yao, Y.P., Hou, W. and Zhou, A.N. (2009), "UH Model: Three-dimensional unified hardening model for overconsolidated clays", *Géotechnique*, **59**(5), 451- 469.

Yao, Y.P., Gao, Z.W., Zhao, J.D. and Wan, Z. (2012), "Modified UH Model: Constitutive modeling of overconsolidated clays based on a parabolic Hvorslev Envelope", *J. Geotech. Geo-environ. Eng*., *ASCE*, **138**(7), 860-868.

GC

Appendix

In this model, the associated flow rule is adopted, i.e., the yield function *f* is equal to the plastic potential function *g*. The yield function *f* is expressed as

$$f = \frac{\lambda - \kappa}{1 + e_0} \ln \frac{p + p_{ri}}{p_x + p_{ri}} + \frac{\lambda - \kappa}{1 + e_0} \ln\left(1 + \frac{q^2}{M^2 (p + p_{ri})^2}\right) - H = 0 \tag{A1}$$

According to Prager's consistent condition

$$df = \frac{\partial f}{\partial \sigma_{ij}} d\sigma_{ij} + \frac{\partial f}{\partial p_{ri}} dp_{ri} + \frac{\partial f}{\partial H} dH = 0 \tag{A2}$$

$$d\varepsilon_{ij}^p = \Lambda \frac{\partial f}{\partial \sigma_{ij}} \tag{A3}$$

The elastic part of the stress-strain relation can be written in the incremental form as

$$d\sigma_{ij} = D_{ijkl}^e d\varepsilon_{kl}^e = D_{ijkl}^e (d\varepsilon_{kl} - d\varepsilon_{kl}^p) \tag{A4}$$

Substituting Eqs. (A3)-(A4), Eqs. (5) and (15) into Eq. (A2) gives

$$\frac{\partial f}{\partial \sigma_{ij}} D_{ijkl}^e (d\varepsilon_{kl} - d\varepsilon_{kl}^p) + \psi\left\langle D_{ijkl}^e (d\varepsilon_{kl} - d\varepsilon_{kl}^p)\delta_{ij}/((2.3 \times 3)p)\right\rangle - \frac{1}{R} \frac{M_f^4 - \eta^4}{M^4 - \eta^4} \Lambda \frac{\partial f}{\partial \sigma_{ij}} \delta_{ij} = 0 \tag{A5}$$

where

$$\psi = \left(\frac{p_x - p}{(p_x + p_{ri})(p + p_{ri})} - \frac{2q^2}{(p + p_{ri})[M^2(p + p_{ri})^2 + q^2]}\right) \exp(-\varepsilon_d^p) \tag{A6}$$

Rearranging Eq. (A5) gives

$$\Lambda = \frac{(\partial f/\partial \sigma_{ij}) D_{ijkl}^e d\varepsilon_{kl} + \psi\left\langle D_{ijkl}^e d\varepsilon_{kl}/(6.9p)\right\rangle}{X} \tag{A7}$$

where

$$X = \frac{1}{R} \frac{M_f^4 - \eta^4}{M^4 - \eta^4} \frac{\partial f}{\partial \sigma_{ij}} \delta_{ij} + \psi\left\langle \frac{1}{6.9p} D_{ijkl}^e \frac{\partial f}{\partial \sigma_{kl}}\right\rangle + \frac{\partial f}{\partial \sigma_{ij}} D_{ijkl}^e \frac{\partial f}{\partial \sigma_{kl}} \tag{A8}$$

The relationship between the stress increment tensors $d\sigma_{ij}$ and the strain increment tensor $d\varepsilon_{ij}$ is given by

$$d\sigma_{ij} = D_{ijkl} d\varepsilon_{kl} \tag{A9}$$

with

$$D_{ijkl} = D_{ijkl}^e - D_{ijmn}^e \frac{\partial f}{\partial \sigma_{mn}} \frac{\partial f}{\partial \sigma_{st}} D_{stkl}^e / X \qquad\qquad (A10)$$

$$D_{ijkl}^e = L\delta_{ij}\delta_{kl} + G(\delta_{ik}\delta_{jl} + \delta_{il}\delta_{jk}) \qquad\qquad (A11)$$

$$G = \frac{E}{2(1+\nu)} = \frac{3(1-2\nu)(1+e_0)p}{2(1+\nu)} \qquad\qquad (A12)$$

$$L = \frac{E}{3(1-2\nu)} - \frac{2}{3}G = \frac{(1+e_0)}{\kappa} - \frac{2}{3}G \qquad\qquad (A13)$$

Substituting Eq. (A11) into Eq. (A10) gives

$$D_{ijkl} = L\delta_{ij}\delta_{kl} + G(\delta_{ik}\delta_{jl} + \delta_{il}\delta_{jk}) - (L\frac{\partial f}{\partial \sigma_{mm}}\delta_{ij} + 2G\frac{\partial f}{\partial \sigma_{ij}})(L\frac{\partial f}{\partial \sigma_{nn}}\delta_{kl} + 2G\frac{\partial f}{\partial \sigma_{kl}})/X \qquad (A14)$$

where

$$\frac{\partial f}{\partial \sigma_{ii}} = \frac{\lambda - \kappa}{1+e_0} \frac{1}{p+p_{ri}} \frac{M^2(p+p_{ri})^2 - q^2}{M^2(p+p_{ri})^2 + q^2} \qquad\qquad (A15)$$

$$\frac{\partial f}{\partial \sigma_{ij}} = \frac{\lambda - \kappa}{1+e_0}\left\{ \frac{M^2(p+p_{ri})^2 - q^2}{M^2(p+p_{ri})^2 + q^2} \frac{\delta_{ij}}{3(p+p_{ri})} + \frac{3[\sigma_{ij} - (p+p_{ri})\delta_{ij}]}{M^2(p+p_{ri})^2 + q^2} \right\} \qquad (A16)$$

Where, D_{ijkl}^e and D_{ijkl} are the elastic and elastoplastic stiffness tensors, respectively; δ_{il} is Kronecker's delta; G and L are Lame's constants; E and ν are elastic modulus and Poisson's ratio, respectively.